

## Lattice QCD with Eight Degenerate Quark Flavors

---

**Xiao-Yong Jin\***

*Department of Physics, Columbia University, New York, NY 10027, USA*

*E-mail: [xj2106@columbia.edu](mailto:xj2106@columbia.edu)*

**Robert D. Mawhinney**

*Department of Physics, Columbia University, New York, NY 10027, USA*

*E-mail: [rdm@physics.columbia.edu](mailto:rdm@physics.columbia.edu)*

We report on simulations of QCD with many flavors of degenerate quarks, the DBW2 gauge action and naive staggered fermions, using the rational hybrid Monte Carlo algorithm. We primarily focus on eight degenerate quark flavors where a variety of values of the coupling constant and quark mass have been used in the simulations. The scaling behavior of the hadron spectrum and the string tension of the heavy quark potential is studied, to probe whether the zero temperature, continuum limit of the theory breaks chiral symmetry.

*The XXVI International Symposium on Lattice Field Theory*

*July 14 - 19, 2008*

*Williamsburg, Virginia, USA*

---

\*Speaker.

## 1. Introduction

It is well known that vector-like gauge theories lose asymptotic freedom if the number of massless fermion species,  $N_f$ , exceeds some critical value  $N_f^*$ , where  $N_f^* = 16.5$  for QCD. For  $N_f$  large, but smaller than  $N_f^*$ , a weak coupling, infrared fixed point exists in the two-loop beta function [1, 2], which indicates that as  $N_f$  is increased from zero an interesting conformal phase may exist [3] before  $N_f$  becomes large enough to lose asymptotic freedom. The range of  $N_f$  where such a conformal phase may exist is referred to as the conformal window, and lattice simulations provide an ideal method to determine the location of this window. Using the Schrödinger functional method, the running of the coupling constant can be measured on the lattice [4], which has given evidence for a conformal window for QCD for  $12 \leq N_f \leq 16$ . Additional studies of the behavior of the finite temperature phase transition as a function of  $N_f$  can be used as a probe into the conformal window [5]. In this paper, we investigate the question of whether  $N_f = 8$  QCD is in the conventional, chirally broken phase of QCD, or in the conformal phase. Previous simulations of eight flavor QCD [6] revealed lattice artifacts for the lattice spacings accessible at that time and prevented a clear statement about the phase of the theory at a single lattice spacing, and no information about the continuum limit. Here we use conventional, zero temperature lattice simulations to measure the chiral condensate and light hadron spectrum for a variety of quark masses and lattice spacings, so we can study the zero quark mass limit and the continuum limit.

## 2. Simulations and results

### 2.1 Choice of algorithm: RHMC

We chose the Rational Hybrid Monte Carlo (RHMC) algorithm [7, 8], because it is exact within machine precision, its software implementation includes many optimizations, and it is extensively used for our other  $2 + 1$  flavor simulations with domain wall and staggered fermions. To check it for our current task, we compared our results from a 4 flavor simulation, done as a 2+2 flavor RHMC simulation (which requires the square root of the staggered fermion determinant) to previous results with  $\Phi$  algorithm [9]. In Tab. 1, the plaquette,  $\langle \bar{\psi}\psi \rangle$ , and masses of 4 meson channels are compared.<sup>1</sup> The plaquette values agree at the  $1 \sigma$  level, while the masses differ by 2 to 3 standard deviations, making it likely that there are long autocorrelation times in the simulations which are not under good control.

### 2.2 Choice of lattice action: Staggered fermions with DBW2 gauge

In this exploratory work, we seek to understand the basic properties of  $N_f = 8$  QCD at zero temperature, in the chiral and continuum limits, which requires simulations at many different parameter values. We have chosen to use the naïve staggered fermion action for its remnant chiral symmetry and its simulation speed. To help control the finite lattice spacing artifacts of staggered fermions, we have used the DBW2 gauge action, which produces smoother gauge fields at the lattice scale, for a given low energy physical scale, than other gauge actions. This smoothing of the gauge field might be expected to decrease the lattice artifacts, which we will address shortly.

<sup>1</sup>In this paper, all numeric values of dimensionful quantities are in lattice unit unless explicitly shown.

Algorithm	$\Phi$	RHMC
Run Length	1000 ~ 4760	1290 ~ 3840
Acceptance Rate	0.87	0.60
Measurement Interval	5	10
Plaquette	0.560130(14)	0.560072(39)
$\langle \bar{\psi}\psi \rangle$	0.0404(1)	0.04105(35)
$m_\pi$	0.3210(40)	0.3127(30)
$m_{\pi_2}$	0.3543(35)	0.3495(41)
$m_\rho$	0.4763(59)	0.4610(31)
$m_{\rho_2}$	0.4777(84)	0.4561(37)

**Table 1:** A comparison between RHMC and  $\Phi$  algorithm results using naive staggered fermions and the Wilson gauge action for  $N_f = 4$ ,  $m_q = 0.015$ ,  $\beta = 5.4$ .

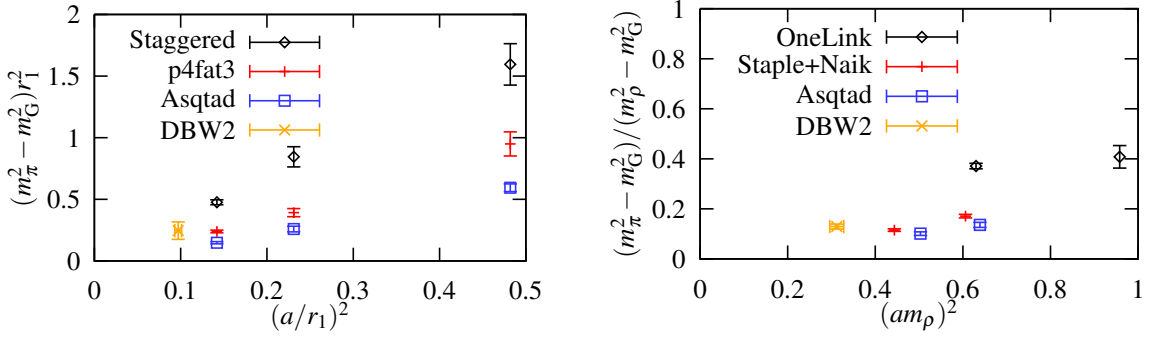


**Figure 1:** A comparison of taste symmetry breaking. Left: compare  $N_f = 2$  DBW2 results with quenched results from [10], where the chiral limit has been taken. Right: compare  $N_f = 2$  DBW2 results with  $N_f = 2$  results from [11, 12] at  $m_\pi/m_\rho = 0.55$ . Here, except for the “DBW2” points, all labels refer to the type of valence quark used on a fixed dynamical ensemble.

Additionally, using the DBW2 gauge action should help to compensate for the coarsening of the gauge fields that comes from adding more fermions. From asymptotic freedom, we know that adding more fermions to a lattice theory with a fixed low energy scale produces a larger coupling at the lattice cutoff, and hence coarser gauge fields. These coarse fields, in turn, make any lattice fermion formulation a poorer approximation to the continuum.

### 2.3 Measuring taste symmetry breaking

We have measured the taste symmetry breaking between the Goldstone pion and the local, non-Goldstone pion for our DBW2 simulations with naïve staggered fermions and 2 dynamical flavors. In Fig. 1, our results are compared with results from improved staggered actions in quenched [10] and 2 flavor (“Staple+Naik” sea quarks with Symanzik improved gauge action) [11, 12] simulations. Although the comparisons are at different lattice spacings, it appears that the DBW2 gauge action has reduced the splittings seen with naive staggered fermions and the Wilson gauge action.

### 2.4 Results with eight flavors

We report on simulations of QCD with 8 degenerate quark flavors with three different values of

$\beta$	Size	$m_q$	Trajectories	$\langle \bar{\psi}\psi \rangle$	$m_p$	$r_0$	$a^{-1}/\text{GeV}$
0.58	$16^3 \times 32$	0.025	1330 ~ 2760	0.09973(27)	0.812(11)	4.39(56)	1.73(22)
		0.015	880 ~ 1950	0.06582(13)	0.619(13)	5.05(78)	1.99(31)
	$24^3 \times 32$	0.025	1060 ~ 3390	0.100381(67)	0.7832(30)	4.126(96)	1.628(38)
		0.015	960 ~ 2930	0.06652(11)	0.6126(28)	5.10(11)	2.014(45)
0.56	$16^3 \times 32$	0.024	970 ~ 4920	0.13643(20)	0.9431(38)	3.19(18)	1.259(70)
		0.016	1040 ~ 3730	0.10147(26)	0.803(12)	3.68(15)	1.451(58)
	$24^3 \times 32$	0.024	1010 ~ 3340	0.13668(14)	0.9693(69)	3.120(48)	1.231(19)
		0.016	1040 ~ 3190	0.10208(12)	0.8085(93)	3.793(97)	1.497(38)
0.54	$16^3 \times 32$	0.03	1010 ~ 6220	0.23100(20)	1.258(17)	2.197(52)	0.867(21)
		0.02	990 ~ 5300	0.19646(28)	1.176(19)	2.350(47)	0.927(19)
		0.01	1030 ~ 5520	0.14464(37)	0.993(14)	2.849(51)	1.124(20)
	$24^3 \times 32$	0.01	1070 ~ 2860	0.14393(39)	1.022(17)	2.830(48)	1.117(19)

**Table 2:** A brief summary of our simulation parameters and results. The value of  $a^{-1}$  is determined from measuring  $r_0$  and assuming  $r_0$  for  $N_f = 8$  has a physical value of 0.5fm.

the coupling:  $\beta = 0.58$ ,  $\beta = 0.56$ ,  $\beta = 0.54$ ; 2 different lattice sizes:  $16^3 \times 32$  and  $24^3 \times 32$ ; and 2 or 3 different values of the quark mass for each coupling. Details can be found in Tab. 2, where the trajectory numbers shown are those trajectories where measurements are done. The length of each trajectory is 0.5 molecular dynamics time units, and measurements are done every 10 trajectories. The jackknife re-sampling method is used throughout our analysis and all the errors we present in this paper are only statistical errors.

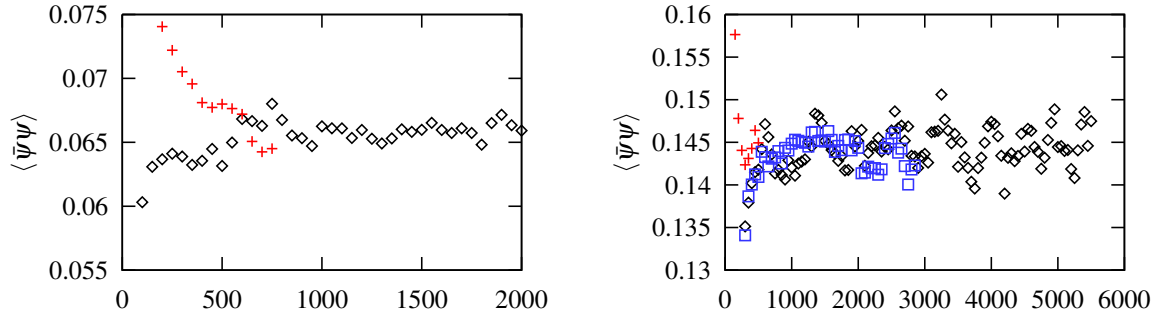
For all three  $\beta$  values, we start our RHMC simulations from both ordered and disordered configurations. In Fig. 2 we show the evolutions of  $\langle \bar{\psi}\psi \rangle$  for  $\beta = 0.58$  and  $\beta = 0.54$ . We see that ordered and disordered starts have values of  $\langle \bar{\psi}\psi \rangle$  which agree after thermalization. The metastability for eight flavor simulations with the Wilson gauge action seen in [6] does not appear in our current work. In addition to the change in action, the earlier work used the inexact R algorithm, while here we use the exact RHMC. While we have not fully investigated what is responsible for the disappearance of metastability, it is very helpful to see that it is not present in the current simulations.

The heavy quark potential is measured on our ensembles using the method in [13], and we fit the potential to the form

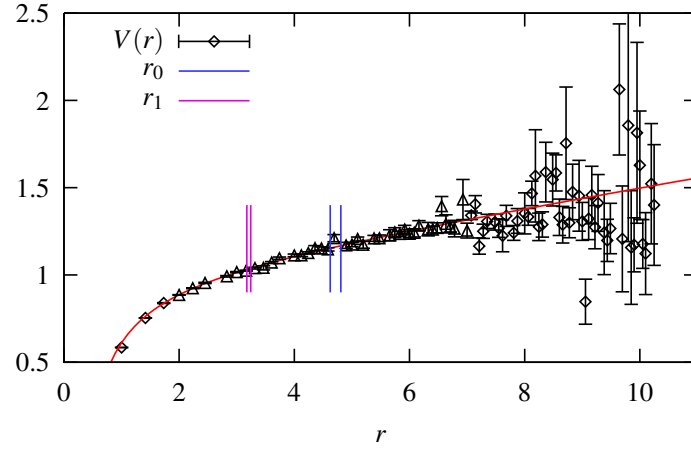
$$V(r) = V_0 - \frac{\alpha}{r} + \sigma r. \quad (2.1)$$

Fig. 3 shows the heavy quark potential for the ensemble with  $\beta = 0.56$ ,  $m_q = 0.008$  on a  $24^3 \times 32$  lattice. The red curve is the fit to Eq. (2.1) over the range of data points denoted by triangle symbols, and the data points shown as diamond symbols are left out of the fit. We can clearly see confining behavior from the shape of the potential. Values of  $r_0$  and  $r_1$  are obtained from the fit and we extrapolate them linearly to the zero quark mass limit as shown in Fig. 4.

It is important to check whether  $N_f = 8$  QCD has dynamical chiral symmetry breaking, which gives  $\langle \bar{\psi}\psi \rangle$  a non-zero value in the zero quark mass limit. In Fig. 5, we show linear extrapolations



**Figure 2:** Evolution of  $\langle \bar{\psi}\psi \rangle$ . Left:  $\beta = 0.58, m_q = 0.015$ . Right:  $\beta = 0.54, m_q = 0.01$ . In both plots, the data is binned in blocks of 50 trajectories. Black diamonds and red crosses represents ordered and disordered starts, respectively, with a lattice size of  $16^3 \times 32$ . Blue squares in the right plot are from an ordered start with a lattice size of  $24^3 \times 32$ .



**Figure 3:** Heavy quark potential measured on ensemble of  $\beta = 0.56, m_q = 0.008$ , with lattice size of  $24^3 \times 32$ .

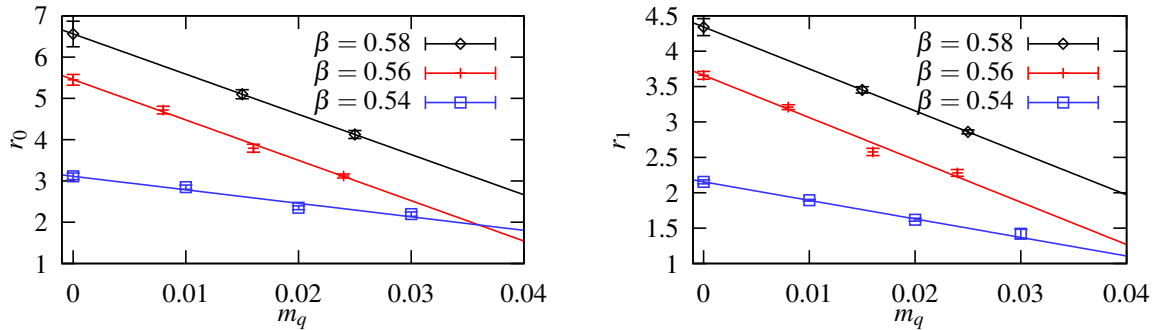


**Figure 4:** Extrapolation to the chiral limit of  $r_0$  and  $r_1$ .

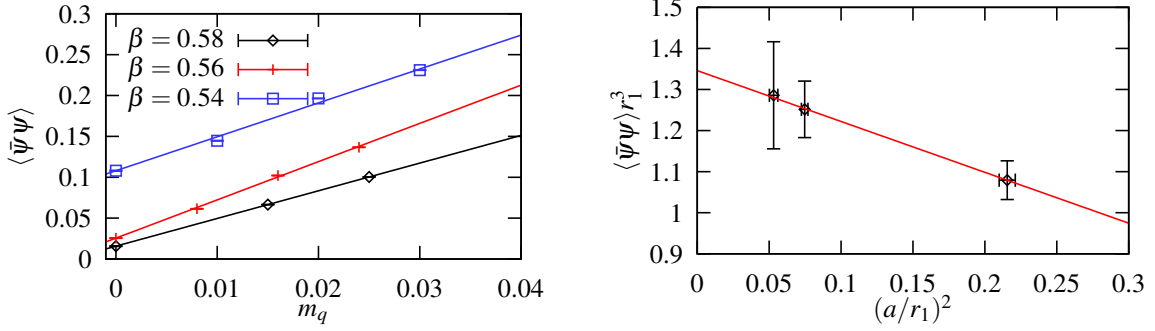


**Figure 5:** The chiral limit extrapolation of the chiral condensate (left panel), and the continuum limit of the chiral limit values.  $\langle \bar{\psi}\psi \rangle$  is not renormalized.

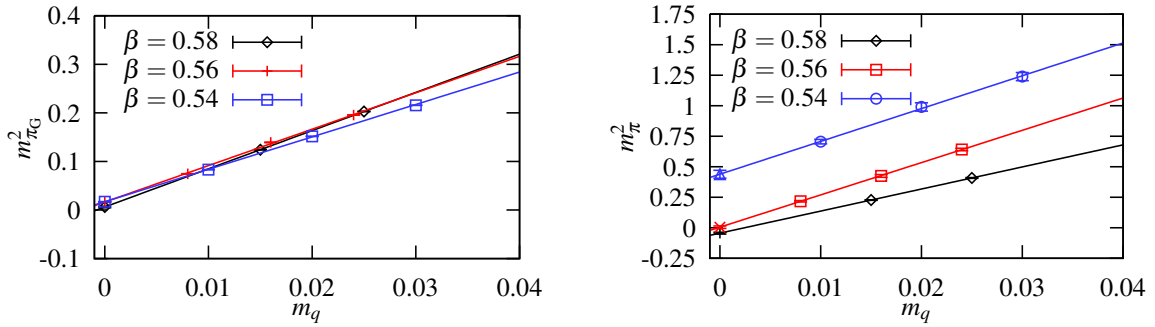


**Figure 6:** Chiral extrapolation of pion mass. Left: Goldstone Pion mass. Right: Non-Goldstone Pion mass – Scalar channel which corresponds to  $r^{\sigma_s \sigma_{123}} = 1++$ , of the meson propagators.

of  $\langle \bar{\psi}\psi \rangle$  to  $m_q = 0$  (left panel) and the scaling behavior of  $\langle \bar{\psi}\psi \rangle(m_q = 0)$  versus  $a^2$  (right panel). The data clearly support a non-zero chiral condensate in the continuum limit.

If  $N_f = 8$  QCD is in a phase with broken chiral symmetry, there should be a pseudo-Goldstone boson whose mass vanishes in the chiral limit. Since staggered fermions have a remnant chiral symmetry, we should be able to see this Goldstone particle in our simulations. We have measured the masses for both the Goldstone pion ( $\pi$ ) and the local non-Goldstone pion ( $\pi_2$ ) in our simulations. In Fig. 6, the left panel shows a linear extrapolation of  $m_{\pi}^2$  versus  $m_q$ . (Clearly there are chiral logarithm corrections to a simple linear extrapolation, but the coefficient of the chiral log term in the continuum goes as  $1/N_f$ , which may make the effects harder to see here than in physical QCD. There are also taste breaking effects in the chiral limit. We have not attempted to include any NLO chiral terms of this kind.) The extrapolated Goldstone mass is consistent with zero, supporting the conclusion that  $N_f = 8$  QCD is in the chirally broken phase. The right panel of Fig. 6 shows the extrapolation of  $m_{\pi_2}^2$  to the chiral limit, which is clearly non-zero for our coarsest lattice. For the finer lattices, the taste-symmetry breaking is much smaller.

We have done a linear extrapolation of our measured values for  $m_\rho$  to the chiral limit, and then extrapolated these to the continuum limit, where we find a non-zero value for  $m_\rho(m_q = 0)$ .

### 3. Conclusions and outlook

We have shown data from lattice simulations of QCD with 8 degenerate quark flavors that supports, in the chiral and continuum limits, a non-zero value for  $r_0$  and  $r_1$  from the heavy quark potential, a non-zero value for  $\langle \bar{\psi}\psi \rangle$ , a massless  $\pi$  and a massive  $\rho$ . This argues that the conformal phase for QCD with  $N_f$  fermions in the fundamental representation must begin with  $N_f > 8$ .

Having presented arguments for the behavior of 8 flavor QCD in the chiral and continuum limits, we are considering looking for evidence of a zero temperature conformal phase in low energy QCD observables with more flavors.

### Acknowledgments

We are thankful to all members of the RBC collaboration for their helpful discussions. Our evolution and propagator measurement code is from Michael Cheng, with minor modifications, and the heavy quark potential measurement code is from Min Li. Our calculations were done on the QCDOC at Columbia University and NY Blue at BNL. This research utilized resources at the New York Center for Computational Sciences at Stony Brook University/Brookhaven National Laboratory which is supported by the U.S. Department, of Energy under Contract No. DE-AC02-98CH10886 and by the, State of New York.

### References

- [1] W. E. Caswell, *Phys. Rev. Lett.* **33** (1974) 244.
- [2] T. Banks and A. Zaks, *Nucl. Phys.* **B196** (1982) 189.
- [3] D. D. Dietrich and F. Sannino, *Phys. Rev.* **D75** (2007) 085018 [[arXiv:hep-ph/0611341](#)].
- [4] T. Appelquist, G. T. Fleming and E. T. Neil, *Phys. Rev. Lett.* **100** (2008) 171607 [[arXiv:0712.0609](#) [hep-ph]].
- [5] A. Deuzeman, M. P. Lombardo and E. Pallante, [arXiv:0804.2905](#) [hep-lat].
- [6] F. R. Brown *et al.*, *Phys. Rev.* **D46** (1992) 5655–5670 [[arXiv:hep-lat/9206001](#)].
- [7] M. A. Clark and A. D. Kennedy, *Nucl. Phys. Proc. Suppl.* **129** (2004) 850–852 [[arXiv:hep-lat/0309084](#)].
- [8] M. A. Clark and A. D. Kennedy, *Phys. Rev. Lett.* **98** (2007) 051601 [[arXiv:hep-lat/0608015](#)].
- [9] C.-Z. Sui, *Flavor dependence of quantum chromodynamics*, . UMI-99-98219.
- [10] M. Cheng *et al.*, *Eur. Phys. J.* **C51** (2007) 875–881 [[arXiv:hep-lat/0612030](#)].
- [11] MILC Collaboration, K. Orginos and D. Toussaint, *Phys. Rev.* **D59** (1999) 014501 [[arXiv:hep-lat/9805009](#)].
- [12] MILC Collaboration, K. Orginos, D. Toussaint and R. L. Sugar, *Phys. Rev.* **D60** (1999) 054503 [[arXiv:hep-lat/9903032](#)].
- [13] M. Li, *PoS LAT2006* (2006) 183 [[arXiv:hep-lat/0610106](#)].